Supporting Information for

Response of online flow cytometry to controlled physicochemical disturbances in desalinated potable water matrixes

Ruisi Chen[a], Theo Huisman[a], Peter Desmond[a,b,*]

[a] College of Science and Engineering, Hamad Bin Khalifa University, Doha, Qatar

[b] Institute of Environmental Engineering, RWTH Aachen University, Aachen, Germany

*Corresponding author, E-mail address: pdesmond@hbku.edu.qa

The residence time distribution (RTD) of the experimental setup was determined using sodium chloride tracer solutions corresponding to conductivities of 500 and 1000 µS/cm (Figure S1.). Each online ICC measurement consisted of four sequential phases: initialization, priming, sampling, and incubation. The tracer was continuously introduced into the system via a syringe pump throughout the sampling phase. Tracer addition was terminated at the onset of incubation. Once the conductivity measured at the drain returned to baseline levels, the drain valve was closed and recirculation to the 18.9 L bottled water container was resumed. The recirculation valve was opened 3 minutes after contaminant addition finished to ensure complete flush out of contaminant from the system and avoid contamination of the feed bottle.

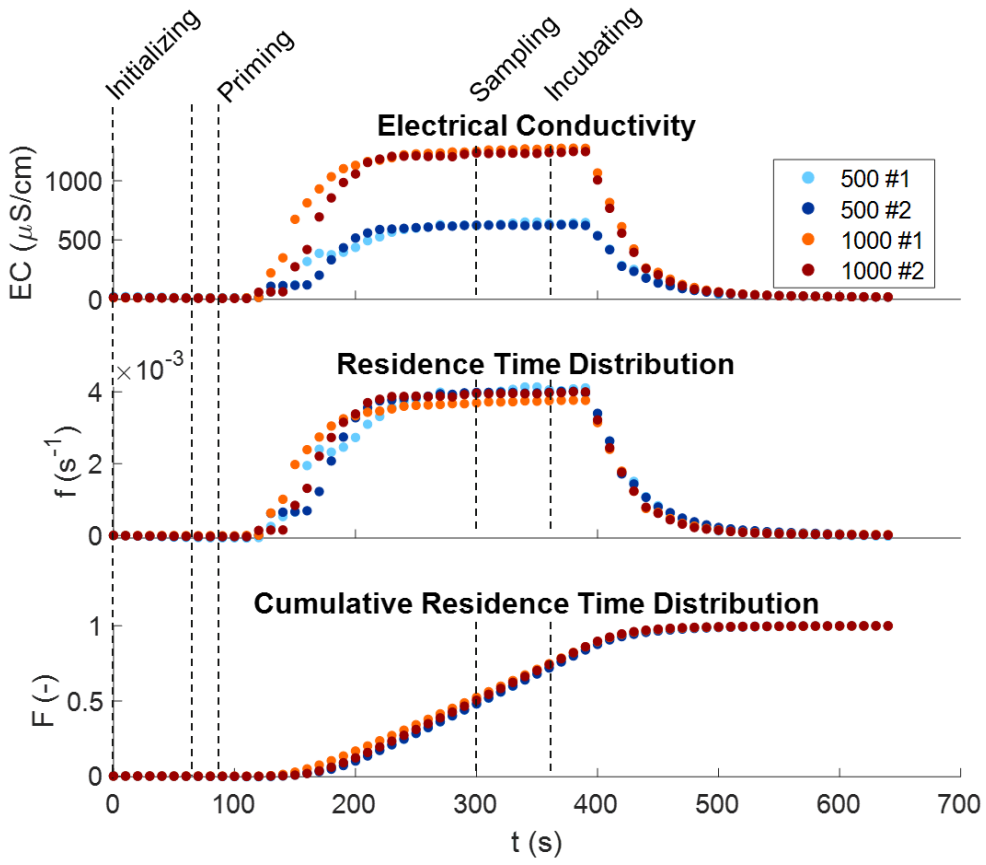

Figure S1. Electrical conductivity, residence time distribution (RTD), and cumulative

residence time distribution of the flow cytometer system as a function of time for duplicates of sodium chloride solutions with conductivities of 500 and 1000 μS/cm.

Table S1. Comparison of previous studies on flow cytometry in water systems and their key limitations

System / Matrix	Real-time monitoring	Disturbance response	Cross-platform comparison	Mechanistic analysis	References (DOI)
Freshwater systems	Laboratory-based FCM analysis	Not investigated	Comparison of offline FCM methods	Gating strategy and signal characterization	10.1016/j.watres.2013.07.051
	Laboratory-based microbial characterization	Not investigated	Not investigated	Fluorescence signal interpretation	10.1016/j.watres.2014.06.020
	Online FCM monitoring of microbial dynamics	Not investigated	Not investigated	Not investigated	10.1016/j.watres.2023.120075
	High-frequency online monitoring in DWDS	Not investigated	Not investigated	Not investigated	10.1016/j.watres.2024.121702
Wastewater reuse systems	Online monitoring combined with ATP	Not investigated	Comparison of FCM and ATP-based indicators	Not investigated	10.1016/j.envint.2019.06.003
	Monitoring in complex reuse systems	Not investigated	Not investigated	Not investigated	10.1016/j.scitotenv.2023.169138
General aquatic systems	Not investigated	Not investigated	Not investigated	Gating strategies and signal processing methods	10.3389/fenvc.2022.931067
NOM-rich systems	Laboratory-based analysis	Organic matter disturbance (single factor)	Not investigated	Fluorescence response to NOM background	10.1016/j.watres.2025.123121
Engineered water systems	Online monitoring in real systems	Not investigated	Not investigated	Not investigated	10.1038/srep38462
	Online monitoring in complex matrices	Not investigated	Cross-platform comparison (sensor integration)	Not investigated	10.1038/s41545-025-00536-5
Desalinated system	Online FCM monitoring under controlled	Systematic evaluation of multi-	Comparison between online and offline FCM	Interpretation of signal variation including gating	This study

System / Matrix	Real-time monitoring	Disturbance response	Cross-platform comparison	Mechanistic analysis	References (DOI)
	conditions	type disturbances (ionic, particulate, organic, chemical)	measurements	and matrix effects	

Table S2. Physicochemical characteristics of influent water

	Tap water	**TSE water**
ICC (cells/mL)	$6.4 \times 10^4 \pm 1245$	$8.4 \times 10^4 \pm 4220$
ATP	14.43 ± 0.15	17.44 ± 0.24
TOC (mg/L)	0.34 ± 0.0189	0.32 ± 0.0422
Turbidity (NTU)	0.12 ± 0.01	0.14 ± 0.02
pH	8.1 ± 0.147	7.2 ± 0.245
EC (μS/cm)	208.2 ± 8.1	212.4 ± 7.2
ORP (mV)	265.24 ± 2.47	276.55 ± 3.45

Table S3. Original concentration and target concentration of controlled disturbances

Original concentration	Injection rate (mL/min)	Target concentration (mg/L)
250000 mg/L NaCl	0.05	50
	0.10	100
	0.25	250
	0.50	500
	1.00	1000
	2.00	2000
	4.00	4000
2000 mg/L Fe_2O_3	0.063	0.50
	0.156	1.25
	0.313	2.50
	0.500	4.00
	0.688	5.50
	0.938	7.50
	1.250	10.00
2000 mg/L Humic acid	0.0125	0.10
	0.0625	0.50
	0.1250	1.00
	0.3125	2.50
	0.6250	5.00
	1.2500	10.00
	3.7500	30.00
10% Citric acid	0.05	33.00
	0.15	100.00
	0.30	200.00
0.5M NaOH	0.10	8.00
	0.50	40.00
	1.00	80.00

Table S4. Typical concentration ranges of selected contaminants in desalinated potable water and TSE

Contaminant	Desalinated potable water (typical)	TSE (typical)
NaCl	5–50 mg/L	100–500 mg/L
Fe_2O_3	<0.05 mg/L (baseline), up to 0.5 mg/L (events)	0.1–1 mg/L
DOC (Humic acid)	<0.5 mg/L	5–20 mg/L
pH (NaOH)	7.5–8.5 (up to >10 events)	6.5–8.5
pH (Citric acid)	negligible	5.5–8.5

Table S5. The dilution factor of the concentrated water matrix and the corresponding syringe pump flow rate

Injection rate (mL/min)	Dilution factor
0.1	2500
0.2	1250
0.3	833
0.4	625
0.6	418
0.8	313
1.0	250

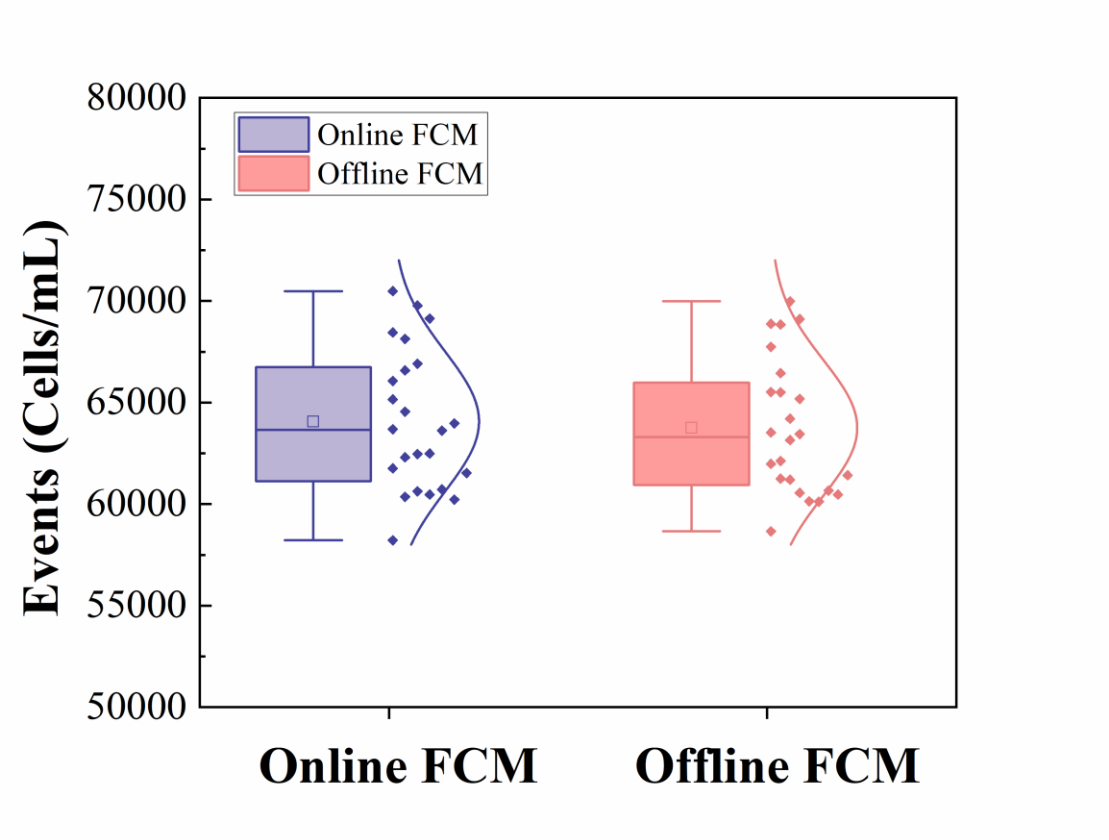

Figure S2. Distributional comparison of ICC measured by online and offline FCM

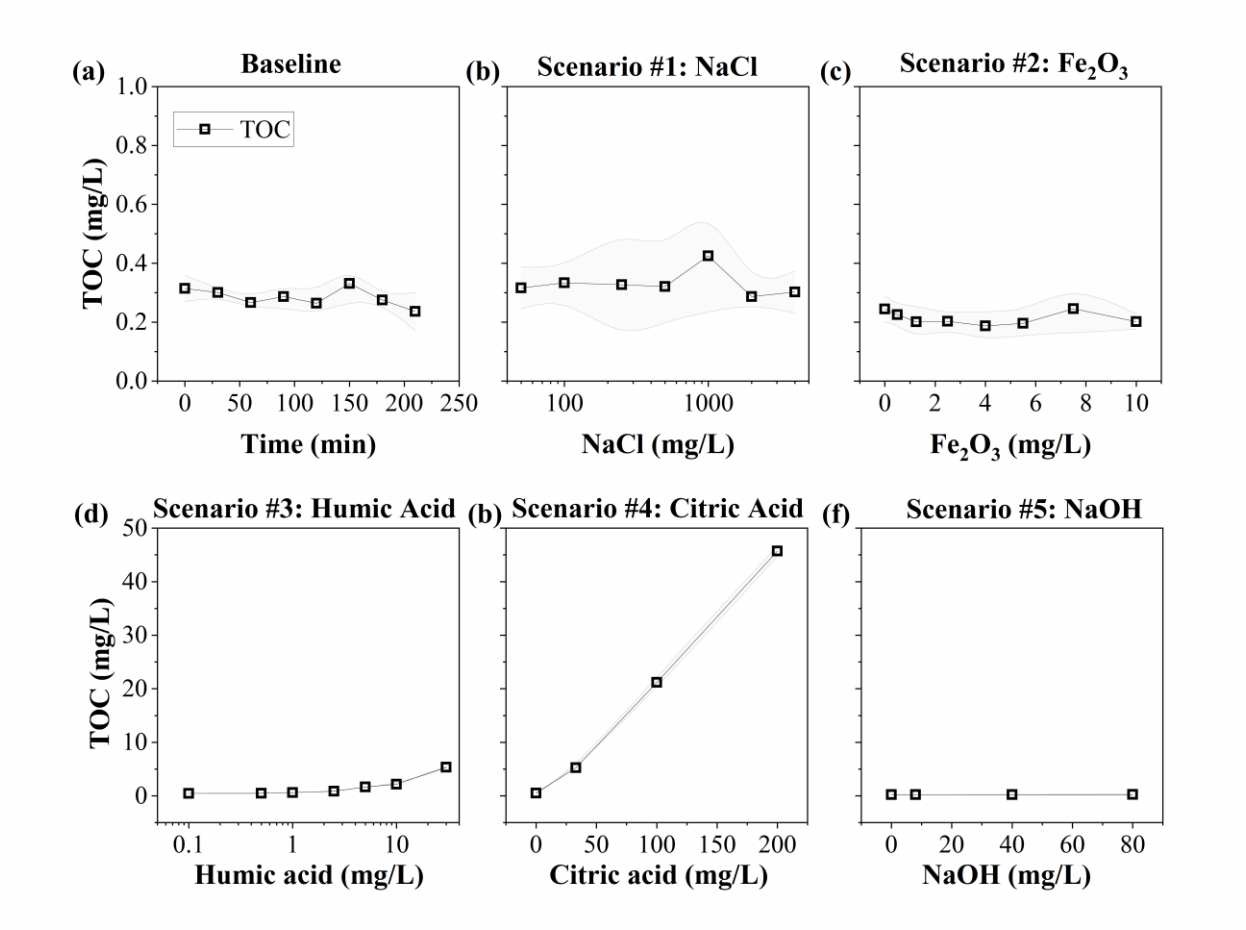

Figure S3. Verification of contaminant addition using total organic carbon (TOC) measurements under different disturbance conditions.
(a) Baseline condition without contaminant addition; (b) NaCl addition; (c) Fe_2O_3 addition; (d) Humic acid addition; (e) Citric acid addition; (f) NaOH addition.

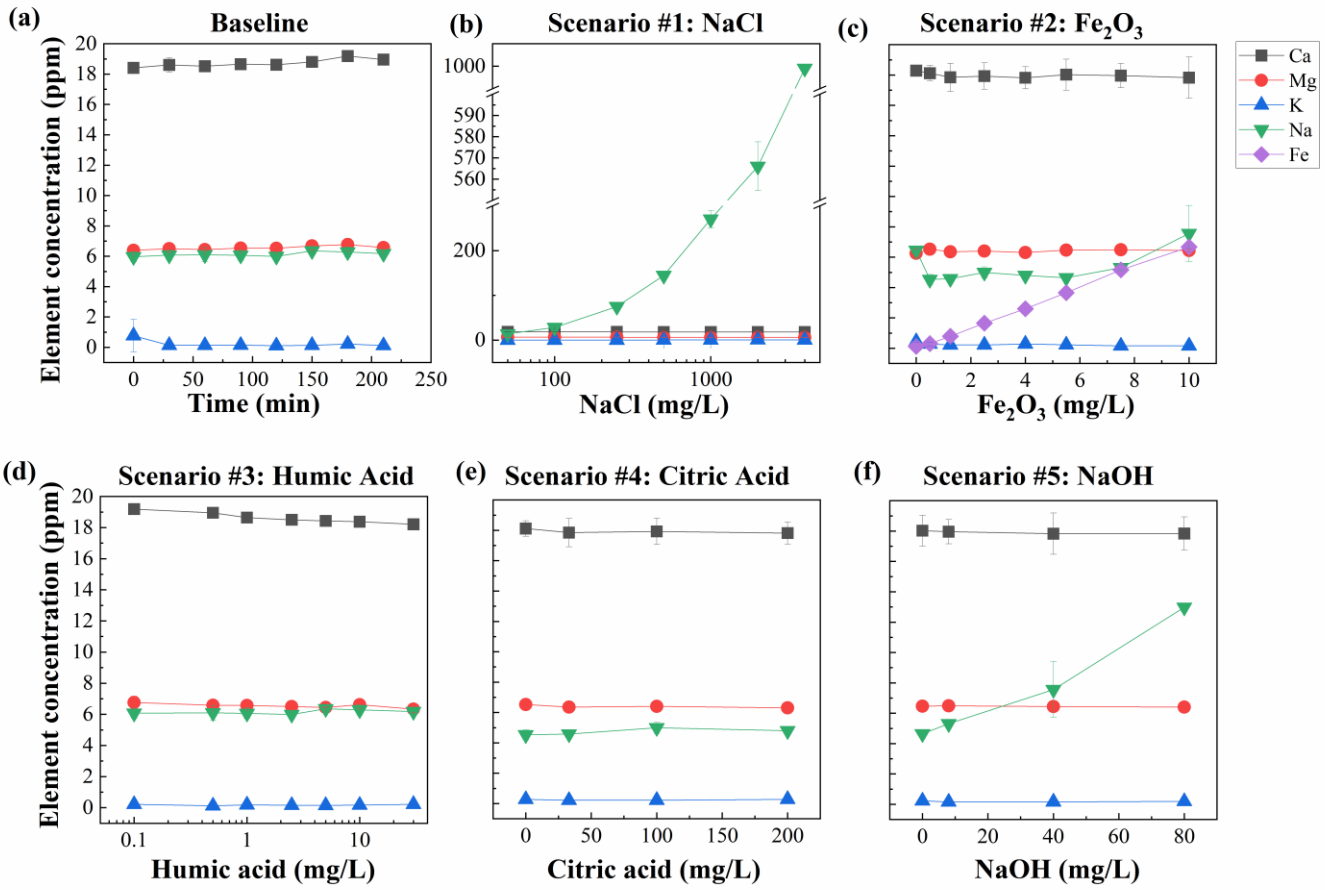

Figure S4. Verification of contaminant addition using inductively coupled plasma optical emission spectrometry (ICP-OES) measurements under different disturbance conditions.

(a) Baseline condition without contaminant addition; (b) NaCl addition; (c) Fe_2O_3 addition; (d) Humic acid addition; (e) Citric acid addition; (f) NaOH addition.

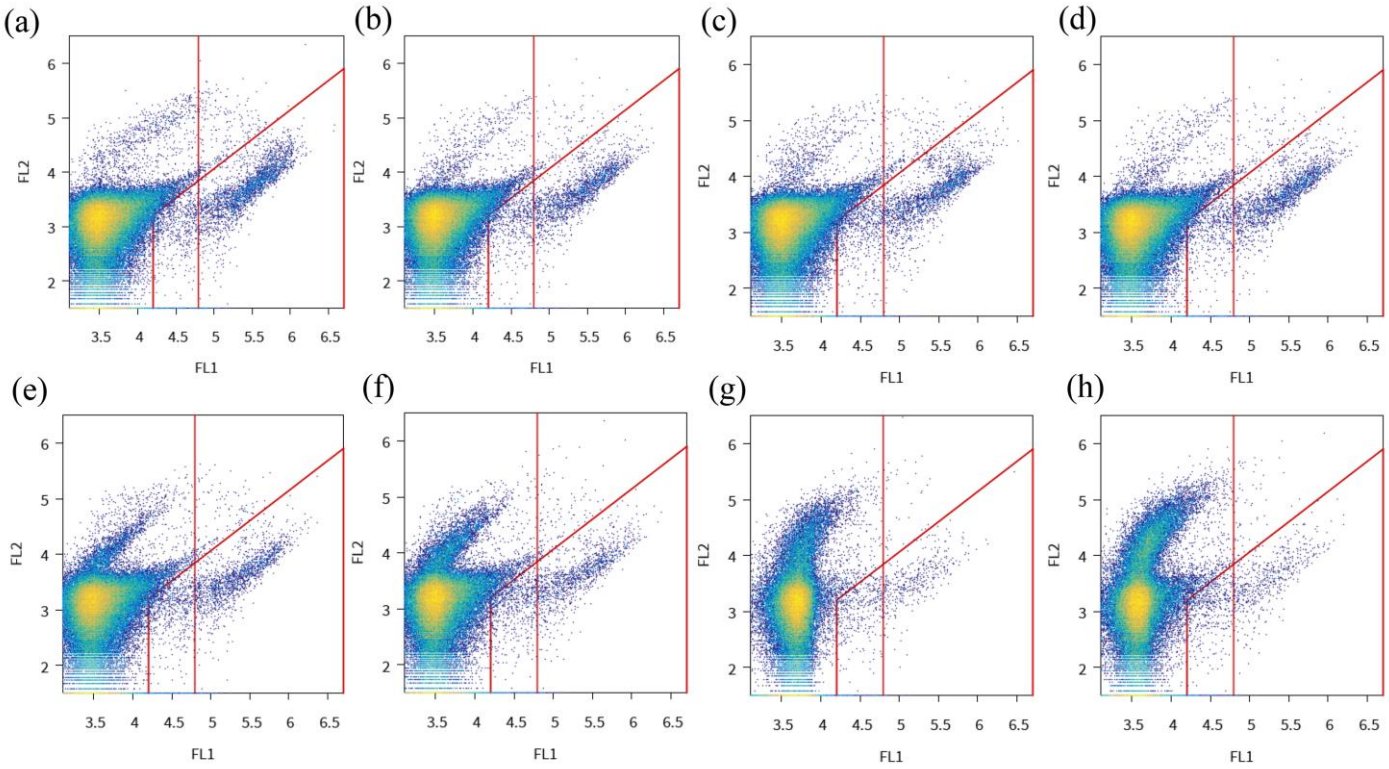

Figure S5. Fluorescence density plots of online flow cytometry (FCM) under increasing concentrations of humic acid.
(a–h) Fluorescence signal distributions at humic acid concentrations of (a) 0 mg/L, (b) 0.1 mg/L, (c) 0.5 mg/L, (d) 1 mg/L, (e) 2.5 mg/L, (f) 5 mg/L, (g) 10 mg/L, and (h) 30 mg/L.

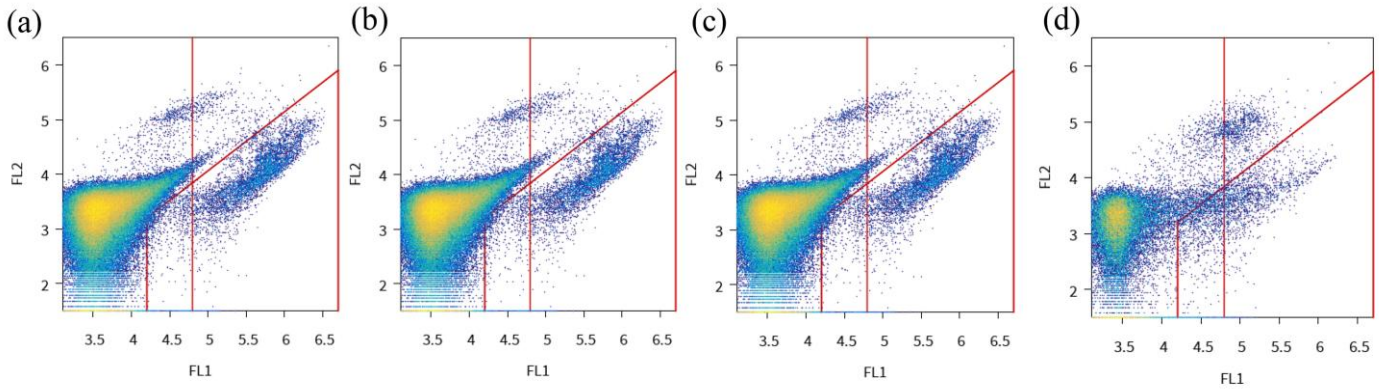

Figure S6. Fluorescence density plots of online flow cytometry (FCM) under increasing concentrations of citric acid.
(a–d) Fluorescence signal distributions at citric acid concentrations of (a) 0 mg/L, (b) 30 mg/L, (c) 100 mg/L, and (d) 200 mg/L.

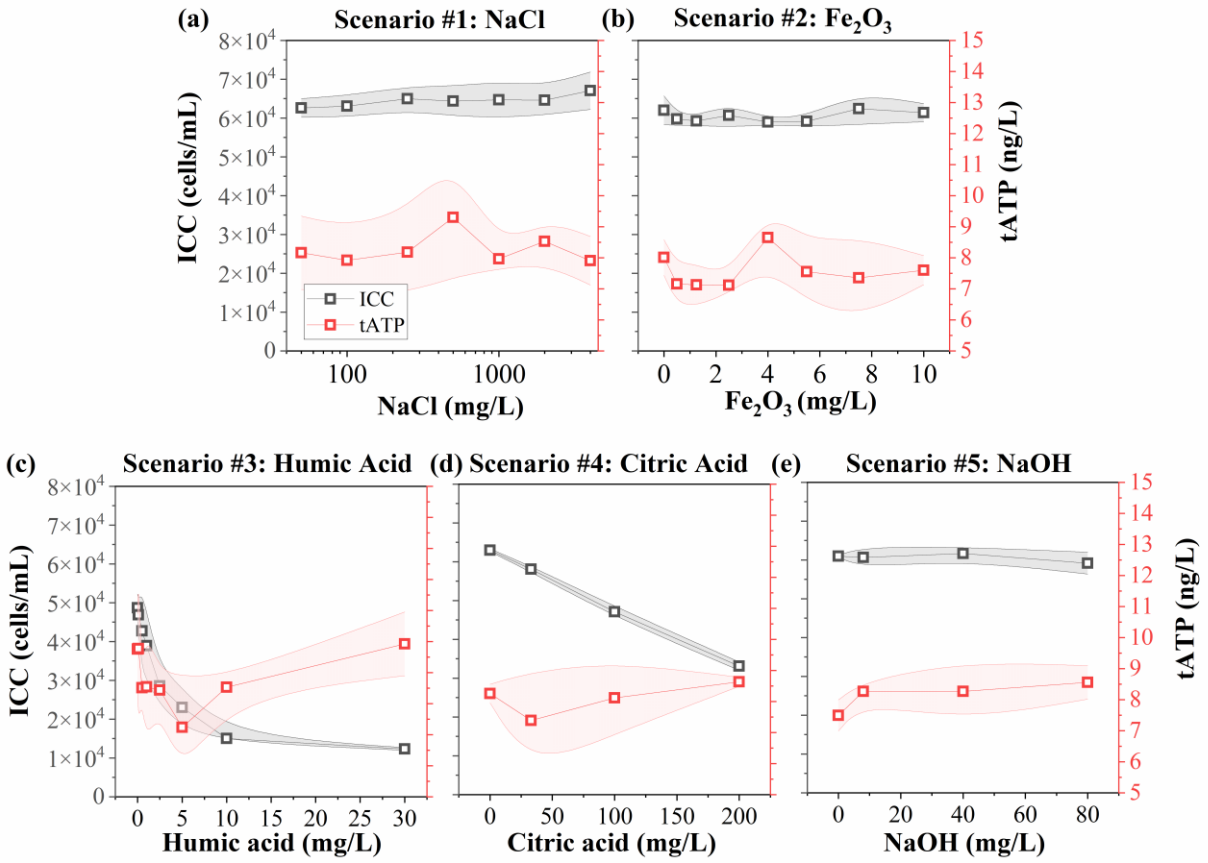

Figure S7. Total ATP (tATP) response under different disturbance conditions. (a–e) tATP concentrations measured under (a) sodium chloride (NaCl), (b) iron oxide (Fe_2O_3), (c) humic acid, (d) citric acid, and (e) sodium hydroxide (NaOH) disturbances.

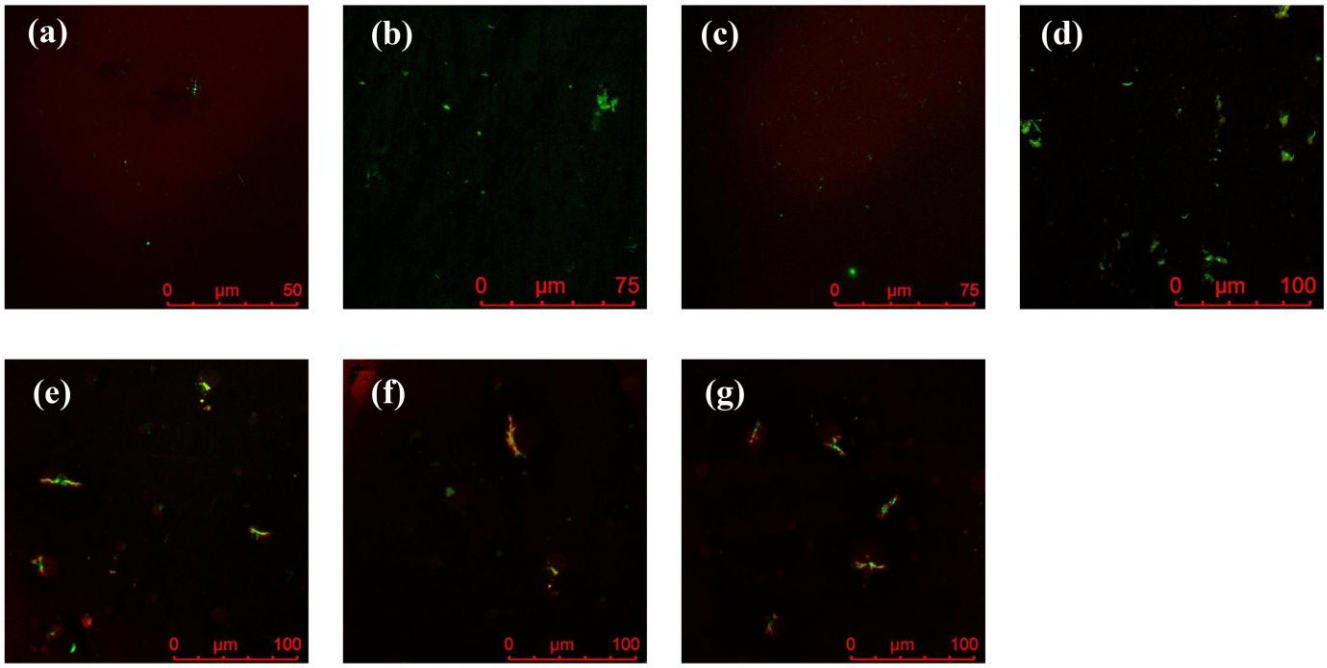

Figure S8. Representative confocal laser scanning microscopy (CLSM) Live/Dead images under different disturbance conditions.
(a) Baseline control using inoculated desalinated water without contaminant addition.
(b–d) Samples exposed to humic acid at concentrations of (b) 1 mg/L, (c) 10 mg/L, and (d) 30 mg/L.
(e–g) Samples exposed to citric acid at concentrations of (e) 33 mg/L, (f) 100 mg/L, and (g) 200 mg/L.
Cells with intact membranes are stained with SYTO 9 and appear as green fluorescence, whereas membrane-compromised or damaged cells are stained with propidium iodide (PI) and appear as red fluorescence.

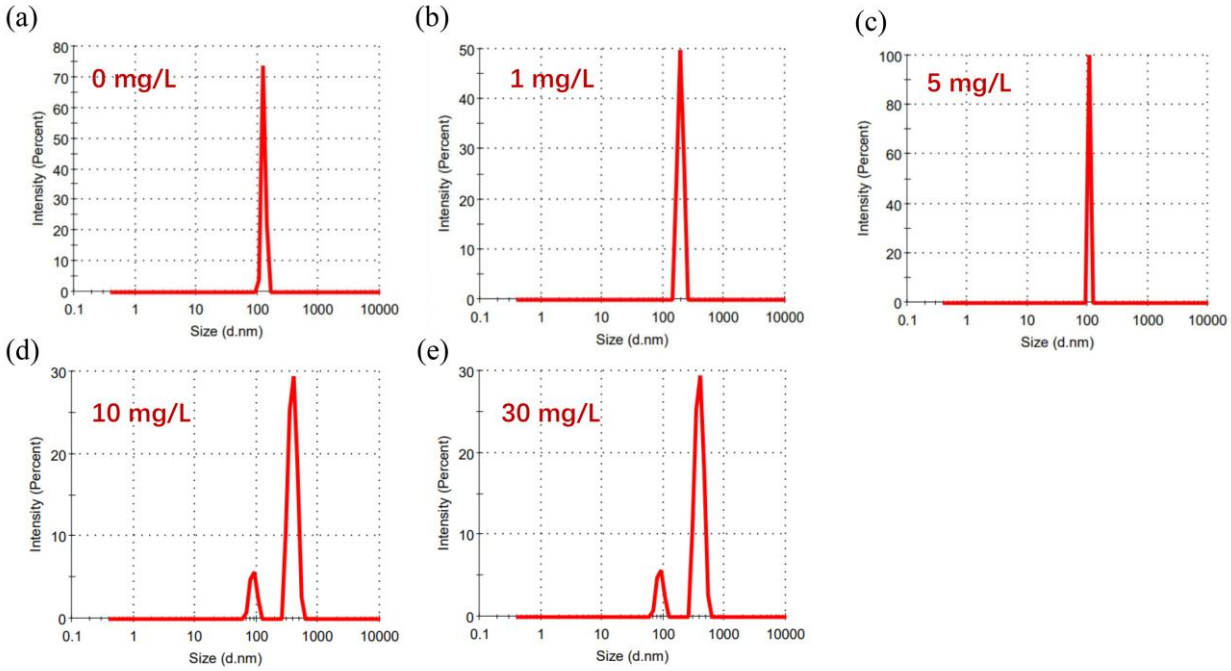

Figure S9. Intensity-weighted hydrodynamic diameter distributions of humic acid particles at increasing concentrations.
(a–e) Particle size distributions measured at humic acid concentrations of (a) 0 mg/L, (b) 1 mg/L, (c) 5 mg/L, (d) 10 mg/L, and (e) 30 mg/L.

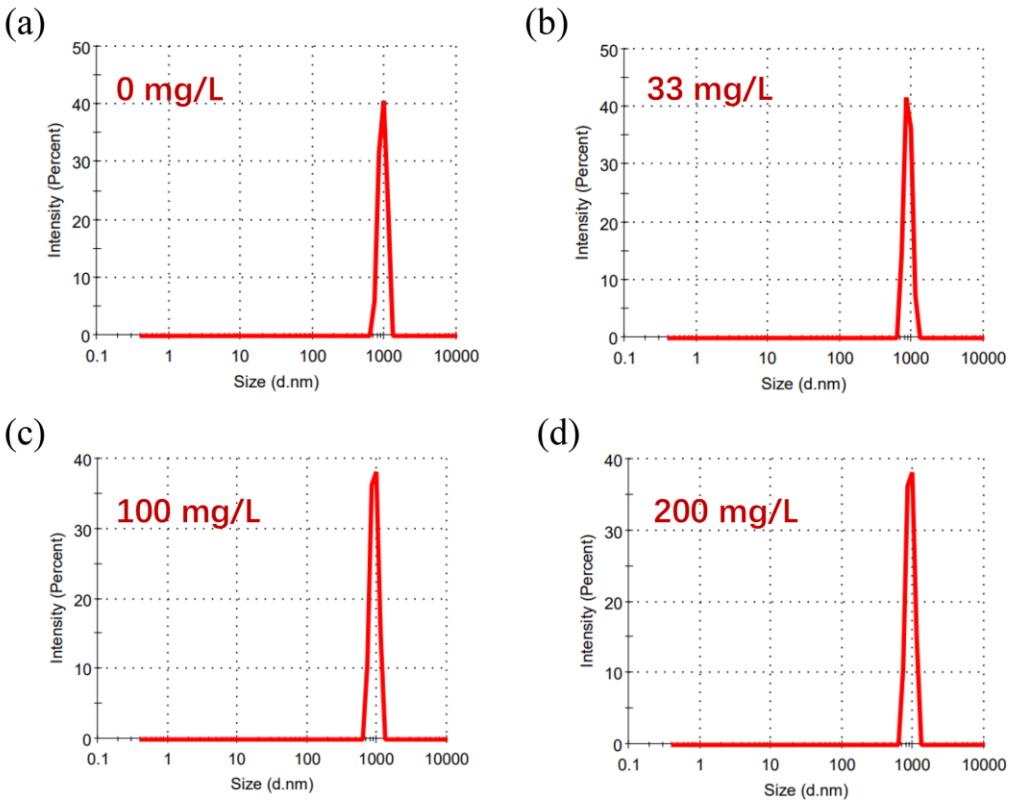

Figure S10. Intensity-weighted hydrodynamic diameter distributions under increasing concentrations of citric acid.
(a–d) Particle size distributions measured at citric acid concentrations of (a) 0 mg/L, (b) 33 mg/L, (c) 100 mg/L, and (d) 200 mg/L.

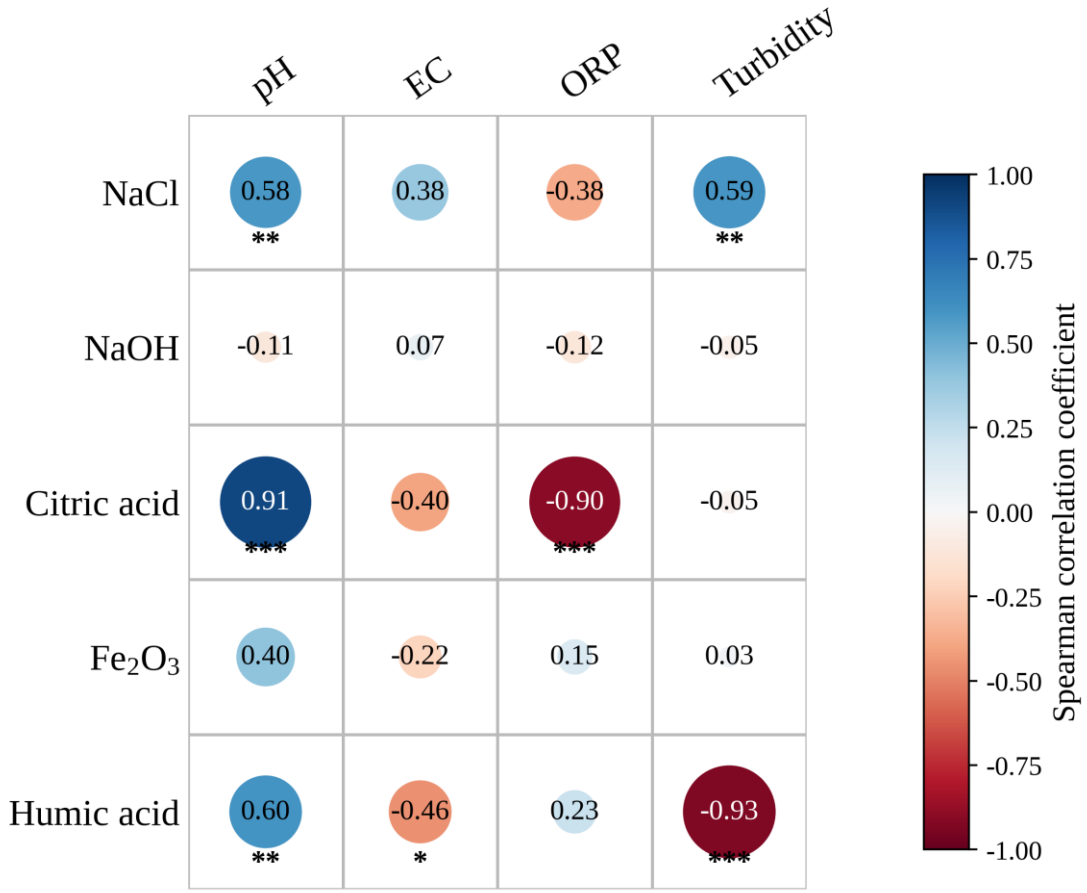

Figure S11. Correlations between ICC and water quality parameters under different scenarios.

Bubble heatmap showing Spearman correlation coefficients between intact cell count (ICC) and selected water quality parameters under different disturbance scenarios. The rows on the left represent the different disturbance scenarios under which ICC was measured. Circle size and color intensity indicate the magnitude of the correlation coefficient, with blue representing positive correlations and red representing negative correlations. Significance levels are indicated as $p < 0.05$ (*), $p < 0.01$ (**), and $p < 0.001$ (***).

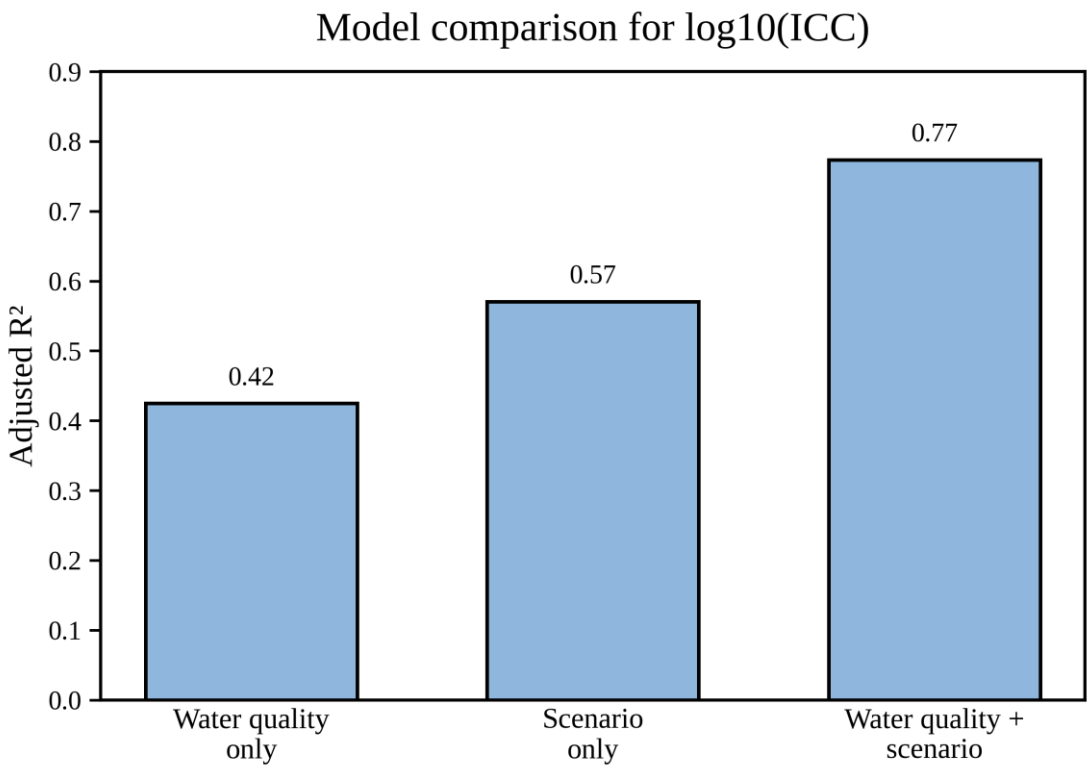

Figure S12. Adjusted R^2 comparison of ordinary least squares regression analysis for ICC variability.

Adjusted R^2 values of regression models using $\log_{10}$-transformed intact cell count (ICC) as the response variable. The three models included water quality parameters only, disturbance scenario only, and both water quality parameters and disturbance scenario. Higher adjusted R^2 indicates stronger explanatory power after accounting for model complexity.

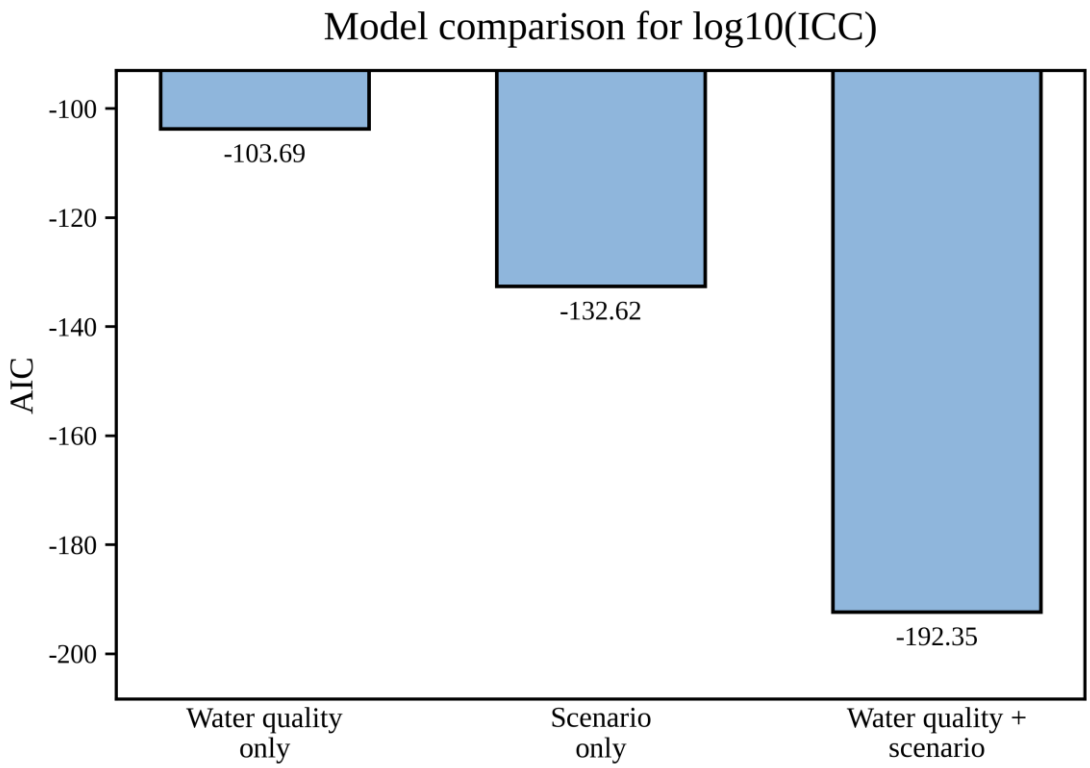

Figure S13. Akaike information criterion (AIC) comparison of ordinary least squares regression analysis for ICC variability.
Akaike information criterion (AIC) values of regression models using $\log_{10}$-transformed intact cell count (ICC) as the response variable. Lower AIC indicates better model performance.